Abnormal behaviors of Goos–Hänchen shift in hyperbolic metamaterials made of aluminum zinc oxide materials

Jing Zhao,[1] Hao Zhang,[1,*] Xiangchao Zhang,[1] Dahai Li,[1] Hongliang Lu,[2] and Min Xu[1]

[1]*Shanghai Ultra-precision Optical Manufacturing Engineering Center, Department of Optical Science and Engineering, Fudan University, Shanghai 200433, China*

[2]*State Key Laboratory of ASIC and System, Department of Microelectronics, Fudan University, Shanghai 200433, China*

Corresponding author: zhangh@fudan.edu.cn

Received August 5, 2013; revised September 27, 2013; accepted October 2, 2013; posted October 2, 2013 (Doc. ID 194899); published November 8, 2013

In this paper, the Goos–Hänchen shift (GHS) at the interface between air and the aluminum zinc oxide (AZO)/ZnO hyperbolic metamaterial (AZO-HMM) is theoretically examined. The results herein show that AZO-HMM can enhance the GHS at the interface to a value at 3 orders of the incident wavelength under special conditions, which is much larger than conventional GHS values. Moreover, the GHS can be tuned to be negative or positive by changing the incident wavelength or the volume fraction of AZO.

OCIS codes: (020.2930) Hyperfine structure; (080.1510) Propagation methods; (160.3918) Metamaterials; (240.6645) Surface differential reflectance.

http://dx.doi.org/10.1364/PRJ.1.000160

1. INTRODUCTION

Recently, stimulated by the prospect of potential applications in superresolution imaging [1], nanophotonic integration, etc., much attention has been paid to a kind of metamaterial called hyperbolic metamaterial (HMM). In addition to the novel dispersion relation of HMM, the reflection of a light beam at the interface when incident from air to HMM also has interesting properties [1,2].

The Goos–Hänchen shift (GHS), as one of the reflection behaviors, was first experimentally observed by Goos and Hänchen in 1947 through a setup that "magnified" the magnitude of the shift through multiple total internal reflections (TIRs) and was subsequently explained by the stationary-phase theory, which was proposed by Artmann [3–5]. In Artmann's theory, the incident beam is expanded into plane-wave components, each with a slightly different transverse wave vector, which undergoes a slightly different phase change after TIR, and, finally, the sum of all the reflected plane waves, i.e., the reflected beam, results in a lateral shift compared to a theoretical path obtained by geometrical analysis of TIR [4]. Usually this shift is extremely small, but it could be enhanced by coupling to a guided mode, or by exciting a preferably low-loss surface electromagnetic wave [4,6]. Large GHS is important in many potential applications, such as optical switches and sensing [7,8]. However, the large losses of conventional materials such as noble metals pose serious limitations on the devices based on GHS.

AZO is one of the transparent conducting oxides (TCOs). Recently, TCOs have attracted much attention in the field of metamaterials due to their applications in the experimental realization of metamaterials [9]. As one kind of new metamaterial, they can be used for sensing, nanoslit lenses, optical cloaking, etc. [8,10]. AZO, indium tin oxide (ITO), and gallium zinc oxide (GZO) are the three main kinds of TCOs. Compared with the other two kinds, AZO has the lowest losses under the same conditions [8].

In this paper, we analyze the GHS of light beams at the interface between air and AZO-HMM. The conditions for large positive and negative shifts are given. It is also found that the lateral optical beam shift depends on the incident angle, the volume fraction of AZO, and incident wavelength. Our numerical results show that GHS of the order of millimeters is possible under special condition and these phenomena are critical for the proposed use in optical sensing, optical switching, etc.

2. THEORY

Supposing a TE-polarized wave is incident to a semi-infinite medium surface, 1 represents air, and 2 is the medium of two-dimensional anisotropic AZO-HMM. The anisotropic dielectric constants of metamaterials can be expressed as

$$\varepsilon_2 = \begin{bmatrix} \varepsilon_{xx} & 0 & 0 \\ 0 & \varepsilon_{yy} & 0 \\ 0 & 0 & \varepsilon_{zz} \end{bmatrix}, \tag{1}$$

where $\varepsilon_{xx} = \varepsilon_{yy} = \varepsilon_{\parallel}$ is the permittivity along the parallel direction and $\varepsilon_{zz} = \varepsilon_{\perp}$ is the permittivity along the normal direction [11]. Herein we consider only nonmagnetic materials, therefore $\mu = 1$. Monochromatic waves can be expressed as follows

$$\mathbf{E} = \mathbf{E}_0 \exp[i(wt - \mathbf{k}\cdot\mathbf{r})], \tag{2}$$

$$\mathbf{H} = \mathbf{H}_0 \exp[i(wt - \mathbf{k}\cdot\mathbf{r})], \tag{3}$$

Considering the continuity of the parallel component of the electric vector $\mathbf{E}$ and magnetic vector $\mathbf{H}$, we have that

$\mathbf{E_{ix}} + \mathbf{E_{rx}} = \mathbf{E_{tx}}$, $\mathbf{H_{iy}} + \mathbf{H_{ry}} = \mathbf{H_{ty}}$ and the expression for the parallel component of k_t can be written as

$$k_{tx} = k_{iz} \tan\theta = (w_2\varepsilon_0\varepsilon_\parallel - w_2\varepsilon_0\varepsilon_1 \sin^2\theta\varepsilon_\parallel/\varepsilon_\perp)^{1/2}, \quad (4)$$

where $\mathbf{E}_{iz}$, $\mathbf{E}_{rz}$, $\mathbf{E}_{tz}$ are the parallel components of the electric field in the incident, reflection, and transmission regions, and similar definitions are given to the case of magnetic field $\mathbf{H}$, as shown in Fig. 1.

Moreover, according to the boundary condition for the electric field at the interface $\mathbf{E_{1y}} = \mathbf{E_{2y}}$, $\mathbf{H_{1x}} = \mathbf{H_{2x}}$, the reflection coefficient can be obtained as follows

$$(1 - r)k_{iz} = tk_{tz}, \quad (5)$$

$$r = (k_{iz} - k_{tz})/(k_{iz} + k_{tz}) = |r| \exp(i\varphi). \quad (6)$$

Similarly, the reflection coefficient for the TM-polarized wave can be obtained as follows:

$$r = (k_{iz}\varepsilon_\parallel - k_{tz}\varepsilon_1)/(k_{iz}\varepsilon_\parallel + k_{tz}\varepsilon_1) = |r| \exp(i\varphi). \quad (7)$$

If the phase of the reflection coefficient is obtained, the GHS can be expressed as follows:

$$\Delta_{\mathrm{GH}} = (k_1 \cos\theta)^{-1} d\varphi/d\theta. \quad (8)$$

For the metamaterial considered herein, which is constructed from alternate layers of AZO material and ZnO, the effective dielectric constant of the composite metamaterial can be obtained by the so-called Maxwell–Garnett effective-medium as follows [11]:

$$\varepsilon_\parallel = f\varepsilon_{\mathrm{AZO}} + (1 - f)\varepsilon_{\mathrm{Al_2O_3}}, \quad (9)$$

$$\varepsilon_\perp = \varepsilon_{\mathrm{AZO}}\varepsilon_{\mathrm{Al_2O_3}}/[(1 - f)\varepsilon_{\mathrm{AZO}} + f\varepsilon_{\mathrm{Al_2O_3}}], \quad (10)$$

where f is the volume fraction of the AZO layers. The effective dielectric constant for the composite metamaterial has a formula similar to that in Eq. (1). Therefore, the dispersion relation for light propagating within the composite metamaterial is written as

$$k_r^2/\varepsilon_\parallel + k_\theta^2/\varepsilon_\perp = w^2/c^2. \quad (11)$$

When $\varepsilon_\parallel > 0$ and $\varepsilon_\perp < 0$, which is called the transverse-positive HMM, the dispersion relationship of the metamaterial is in a hyperbolic shape and can be used in a hyperlens with imaging resolution beyond the diffraction limit [1,2].

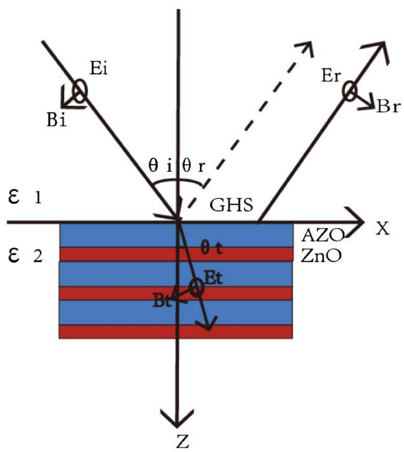

Fig. 1. Schematic of reflections for TE-polarized incident waves at the interface between an isotropic medium and an anisotropic medium.

Table 1. Parameters of AZO Samples

Samples	Volume Fraction of Al	Number of Cycles of Al_2O_3	Number of Cycles of ZnO	Number of Macrocycles	Total Thickness [nm]
1	1%	1	49	5	49.5
2	2%	1	25	10	51
3	10%	1	5	40	44

3. RESULTS AND DISCUSSION

In our experiment, we used the atomic layer deposition (ALD) method for the preparation of AZO samples. Because of continued device miniaturization, control of thin-film growth is needed at the atomic level to fabricate semiconductor and other nanoscale devices [12,13]. We alternatingly pulse the precursors diethylzinc (DEZ) and trimethylaluminum (TMA). Al is pulsed after N cycles of ZnO. We prepare three AZO samples with different volume fractions of Al_2O_3, namely, Al, 1%; Al, 2%; and Al, 10%. The thickness of one cycle of Al_2O_3 is 0.1 nm and the thickness of ZnO is 0.2 nm. The detailed parameters are shown in Table 1.

The permittivity of AZO was measured using a spectroscopic ellipsometer. The optical constants were extracted using a Drude–Lorentz model [8,14]. Figure 2 shows the

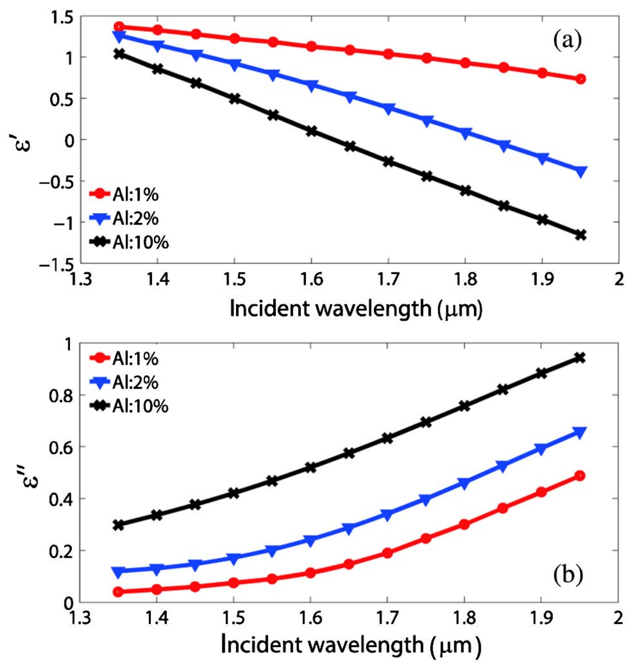

Fig. 2. (a) Real permittivity of AZO in the near-IR. (b) Imaginary permittivity of AZO in the near-IR.

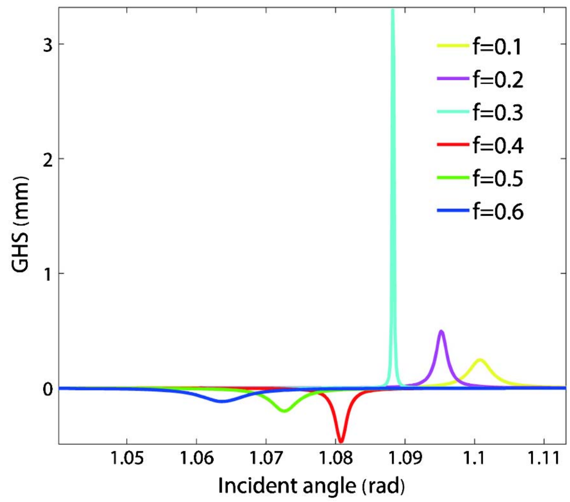

Fig. 3. Dependence of GHS on incident angles for different volume fractions of AZO (Al: 2%). $\lambda = 1.9$ μm.

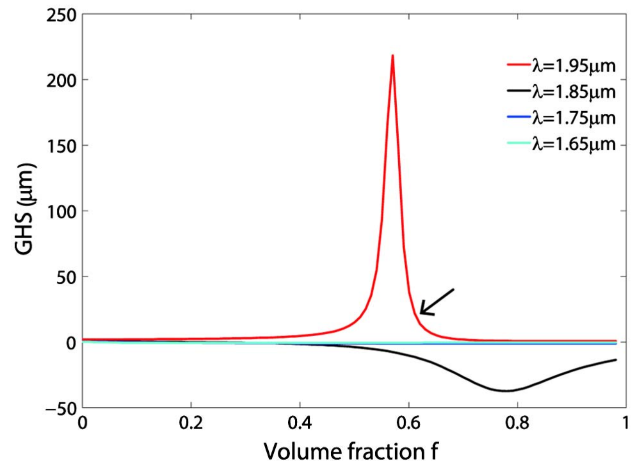

Fig. 5. Dependence of GHS on the volume fractions of AZO for different incident wavelengths and a fixed incident angle, $\theta = 60°(\sim 1.05\,\text{rad})$. The arrow indicates the configuration used for the numerical simulation in Fig. 6.

dielectric constants of the AZO samples. We find that in the near-IR range, AZO shows negative real permittivity and positive imaginary permittivity. The real permittivity of the samples declines with the rise of the volume fraction of Al under the same incident wavelength. The imaginary part has the opposite trend.

The curves of the corresponding GHS and the incident angle for different volume fractions of AZO-doped ZnO films are shown in Fig. 3. The curves of the corresponding GHS and the incident angle for different incident wavelengths are shown in Fig. 4.

In order to study the dependence of GHS on the volume fraction of AZO, the incident angle is fixed to be 60° and the corresponding GHS for different volume fractions of AZO is obtained, as shown in Fig. 5.

We use the finite-element method to calculate the snapshot of the normalized magnetic field for AZO-HMM, which is shown in Fig. 6. The incident wavelength λ is equal to 1.95 μm and the dielectric constant of the AZO-HMM is equal to $(1.8810 + 0.3306i, -0.6658 + 11.1072i)$. By simulation, it is obtained that $\Delta_{\mathrm{GH}} \approx 21.1$ μm, which is approximately equal to the theoretical value of 21.9 μm (indicated by the arrow in Fig. 5).

By theoretical calculations, it is found that the GHS occurring at the interface between the metamaterial film and air is influenced by the incident angle θ, incident wavelength λ, and the volume fraction f of AZO.

As Fig. 3 shows, when $\lambda = 1.9$ μm and $f \leq 0.3$, GHS is positive and can be enhanced as large as above 3 mm ($f = 0.3$); when $f > 0.3$, the GHS is tuned to be negative. In Fig. 4, when $f = 0.37$ and $\lambda \leq 1.75$ μm, GHS is positive and it is switched to negative when $\lambda > 1.75$ μm. Therefore, for the metamaterial film constructed by AZO/ZnO, the GHS at the interface can be continuously tuned from a large positive value to a large negative value by changing the volume fraction or incident wavelength, which provides promising novel applications in

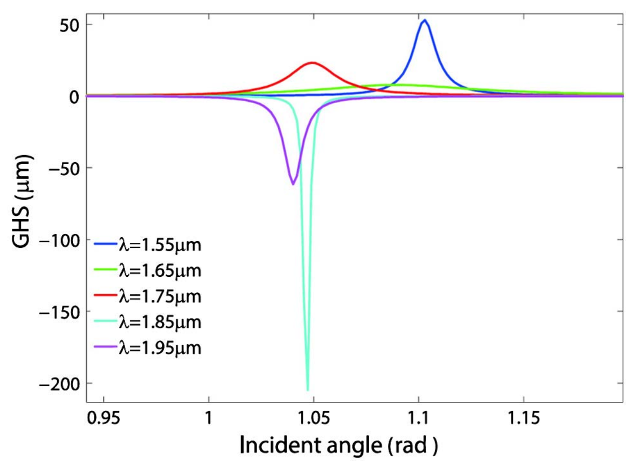

Fig. 4. Dependence of GHS on incident angles for different incident wavelengths. $f = 0.37$.

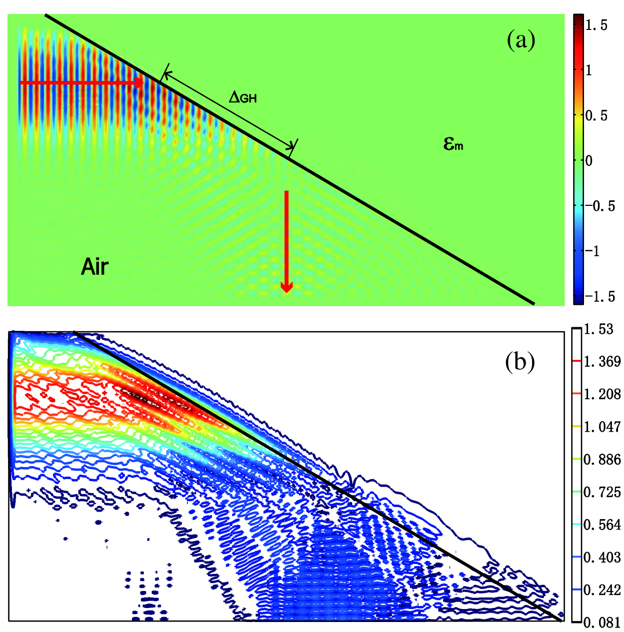

Fig. 6. (a) Snapshots of the normalized magnetic field and (b) the normalized energy flux of the magnetic field for an incident beam at $\lambda = 1.95$ μm. The angle of the AZO-HMM slope is $\theta = 60°$.

the fields of optical sensors, optical switches, etc. [7,8,15]. Additionally, the study of optical properties like GHS can also contribute to designing better metamaterials [1,16].

4. CONCLUSION

In conclusion, the values of GHS at the AZO-HMM interface are generally 1 order of magnitude comparable to the wavelength. However, it is demonstrated herein that a millimeter-scale GHS can be reached under special conditions. The GHS is shown to be very sensitive to the incident wavelength and the volume fraction of AZO. AZO-HMM can be used to overcome the problem caused by large losses for conventional metals in the design of optical devices based on the GHS mechanism and enable many potential applications, such as optical sensing and optical switches.

ACKNOWLEDGMENTS

This work is supported in part by the National High Technology R&D Program of China (863 Program) under Grant No. 2012AA040406 and the National Natural Science Foundation of China under Grant No. 11374063.

REFERENCES

1. H. W. Liu, H. Lee, Y. Xiong, C. Sun, and X. Zhang, "Far-field optical hyperlens magnifying sub-diffraction-limited objects," Science **315**, 1686 (2007).
2. X. J. Ni, S. Ishii, M. D. Thoreson, and V. M. Shalaev, "Loss-compensated and active hyperbolic metamaterials," Opt. Express **19**, 25242–25254 (2011).
3. K. Artmann, "Calculation of the lateral displacement of a totally reflected ray," Ann. Phys. **2**, 87 (1948).
4. Y. H. Wan, Z. Zheng, and W. J. Kong, "Nearly three orders of magnitude enhancement of Goos-Hänchen shift by exciting Bloch surface wave," Opt. Express **20**, 8998–9003 (2012).
5. K. Y. Bliokh and A. Aiello, "Goos-Hänchen and Imbert-Fedorov beam shifts: an overview," J. Opt. **15**, 014001 (2013).
6. M. Ornigotti and A. Aiello, "Goos-Hänchen and Imbert-Fedorov shifts for bounded wavepackets of light," J. Opt. **15**, 014004 (2013).
7. X. P. Wang, C. Yin, and J. J. Sun, "Reflection-type space-division optical switch based on the electrically tuned Goos-Hänchen effect," J. Opt. **15**, 014007 (2013).
8. G. V. Naik, J. Kim, and A. Boltasseva, "Oxides and nitrides as alternative plasmonic materials in the optical range," Opt. Mater. Express **1**, 1090–1099 (2011).
9. X. B. Liu, Z. Q. Cao, P. F. Zhu, Q. S. Shen, and X. M. Liu, "Large positive and negative lateral optical beam shift in prism-waveguide coupling system," Phys. Rev. E **73**, 056617 (2006).
10. G. V. Naik and A. Boltasseva, "A comparative study of semiconductor-based plasmonic metamaterials," Metamaterials **5**, 1–7 (2011).
11. O. Kidwai, S. V. Zhukovsky, and J. E. Sipe, "Effective-medium approach to planar multilayer hyperbolic metamaterials: strengths and limitations," Phys. Rev. A **85**, 053842 (2012).
12. S. M. George, "Atomic layer deposition: an overview," Chem. Rev. **110**, 111–131 (2010).
13. G. N. Parsons, S. M. George, and M. Knez, "Progress and future directions for atomic layer deposition and ALD-based chemistry," MRS Bull. **36**, 865–871 (2011).
14. G. V. Naik, J. J. Liu, and A. V. Kildishev, "Demonstration of Al:ZnO as a plasmonic component for near-infrared metamaterials," Proc. Natl. Acad. Sci. USA **109**, 8834–8838 (2012).
15. L. Y. He, Z. Q. Biao, and Z. Yan, "Opposite Goos-Hanchen displacement for TE- and TM-polarized beams transmitting through a slab of indefinite metamaterial," Chin. Phys. Lett. **27**, 074210 (2010).
16. Y. M. Liu and X. Zhang, "Metamaterials: a new frontier of science and technology," Chem. Soc. Rev. **40**, 2494–2507 (2011).